THE JOURNAL OF PHYSICAL CHEMISTRY Letters

Perspective

pubs.acs.org/JPCL

Porous Metal–Organic Frameworks for Gas Storage and Separation: What, How, and Why?

Bin Li,[†] Hui-Min Wen,[†] Wei Zhou,[‡,§] and Banglin Chen*[,†]

[†]Department of Chemistry, University of Texas at San Antonio, San Antonio, Texas 78249, United States

[‡]NIST Center for Neutron Research, National Institute of Standards and Technology, Gaithersburg, Maryland 20899-6102, United States

[§]Department of Materials Science and Engineering, University of Maryland, College Park, Maryland 20742, United States

ABSTRACT: Metal–organic frameworks (MOFs) have been emerging as promising multifunctional materials and have shown particularly useful applications for gas storage and separation. We have briefly outlined the early development of this very active research field to provide us a clear picture on what are MOFs and how the research endeavor has been initiated and explored. Following that, we have demonstrated why MOFs are so unique for gas storage and separation: high porosities, tunable framework structures, and immobilized functional sites to fully make use of pore space for gas storage, to optimize their sieving effects, and to differentiate their interactions with gas molecules. Finally, we have provided a perspective on further development of porous MOFs for gas storage and separation.

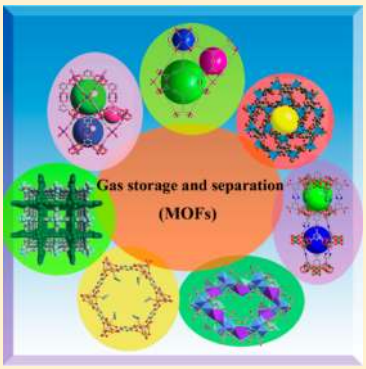

The last two decades have witnessed the emerging of functional metal–organic framework (MOF) materials.[1] Such materials can be easily self-assembled from their corresponding metal ions/clusters with organic linkers.[2] Because a variety of different chemically, optically, magnetically, electrochemically, biologically, and catalytically active metal ions/clusters and organic linkers can be incorporated into such framework materials, whereas their porosities have enabled them to encapsulate a number of different guest substrates such as gases, ions, nanoparticles, biological chemicals, and dyes, this new type of inorganic–organic hybrid materials has wide applications on gas storage, separation, sensing, catalysis, drug delivery, nonlinear optics, lasing, and data storage.[3−9]

> A brief overview on the early development of this very active research field provides us a clear picture on what are MOFs and how the research endeavor has been initiated and explored.

It is interesting to briefly overview the development of this very active research field, so we can learn from the history on how a new research endeavor has been initiated and explored exponentially even beyond our imagination. In the early 1990s, research has been mainly focused on the syntheses, X-ray crystal structures, and topological rationalization of coordination polymers (CPs) or coordination networks (CNs) by scientists Robson, Zaworotko, and Ciani et al. within crystal engineering community though potential applications for molecular sieving and ion exchange have been proposed.[10−12] Given the fact that (a) a few coordination complexes, for example, $Ni(4\text{-}MePyridine)_4(NCS)_2$, can take up gas/vapor molecules,[13] (b) single-crystal X-ray structures of a few coordination polymers have been established to have framework structures,[14] (c) a large number of inorganic linkers such as O^{2-}/OH^- in porous zeolite materials,[15] CN^- in Prussian Blue,[16] and phosphates and sulfides[17] in other type of porous materials, it seems to be quite natural to foresee the potential of such coordination polymers as porous materials. However, it took a long time to eventually establish the permanent porosities of the first several coordination polymers because of the difficulty to stabilize the frameworks that can survive under thermal/vacuum activation. The frameworks which can retain their crystalline features through solvent guest exchanges were realized by Lee and Yaghi independently in 1995 by making use of the very similar guest solvents such as C_6D_6 to replace C_6H_6 in $[Ag(TEB)CF_3SO_3]\cdot(C_6H_6)_2$ and $C_6H_5NO_2$, C_6H_5CN, and C_6H_5Cl to replace pyridine in $CoC_6H_3(COOH_{1/3})_3(NC_5H_5)_2\cdot 2/3NC_5H_5$.[18,19] It was also in 1995 (Yaghi), for the first time, termed the metal–organic framework and showed that this framework can survive thermal activation at 200 °C for 6 h to retain its framework crystalline nature, as confirmed by powder XRD.[20] At the same time, Lee and Moore established that $Ag(\mathbf{1})(CF_3SO_3)]\cdot 2C_6H_6$ (**1** = 1,3,5-tri(3-ethynylbenzonitrile)benzene) can survive gentle thermal activation at 110 °C for 10 min through unit cell

Received: July 29, 2014
Accepted: September 25, 2014
Published: September 25, 2014

determination and PXRD studies.[21] Subsequently, Yaghi established porous MOFs $M_3(BTC)_2{\cdot}12H_2O$ (M = Co^{2+} and Zn^{2+}), which can reversibly take up water and ammonia molecules in 1996.[22] The breakthrough was eventually realized during 1997−1999 in which a few porous coordination polymers have been exclusively established experimentally for gas sorption isotherms: Kitagawa established the high pressure gas sorption isotherms of $M_2(4,4'\text{-bpy})_3(NO_3)_4$[23] in 1997 and Yaghi realized the gas sorption properties of Zn(BDC)[24] (**MOF-2**) in 1998. The one, **MOF-5** (later on also termed as **IRMOF-1**), discovered by Yaghi,[25] immediately attracted wide attention because of its extremely high porosity with BET over 3000 $m^2\ g^{-1}$. In 1999, Rosseinsky and Yaghi independently and exclusively established the pore structures of two MOFs by single X-ray diffraction studies.[26] Apparently, it is high porosities of such framework materials that distinguish themselves from other traditional porous materials such as zeolites and activated carbons. Since the early 2000s, the term "metal−organic framework" has been widely utilized simultaneously with "coordination polymers" or other similar terms such as "coordination networks", "metal−organic coordination networks". Scientists have been developing the research on MOF/CP materials from different perspective, it is understandable that they would prefer to use one term over another. As suggested by IUPAC,[27] "metal−organic framework" was subclass of "coordination polymers" with void spaces to "highlight those stable porous coordination polymers, and to emphasize the similarity of these special types of coordination polymers with those traditional porous solid materials in terms of their framework structures, topologies and properties. Essentially, porous coordination polymer and metal−organic framework have the same meanings, which are defined from two different perspectives: the term "porous coordination polymer" emphasizes the bonding nature between metal ions and bridging organic linkers and structurally polymeric features from the chemistry point of view; whereas the term "metal−organic framework" highlights the similarity with traditional framework solids, particularly zeolite framework materials and, thus, emphasizes the robustness and the porosity from the material point of view."[2]

The syntheses of MOFs were established in early 2000s as well, as exemplified in the solvothermal synthesis of **MOF-14**.[28] Further extensive studies on the construction and exploration of MOFs have motivated Yaghi and O'Keeffe to establish the reticular chemistry for MOF materials, which to certain extent has enabled us to rationally design and construct porous MOFs of specific porosities and functions. Porous MOFs have some unique features for gas storage and separation: (1) extremely high porosities which can be up to 7000 m^2/g, (2) tunable framework structures and porosities, (3) rationally immobilized functional sites and pores surfaces. Herein, we highlight the current status of porous metal−organic frameworks on gas storage and separation.

Porous MOFs with High Porosities for Gas Storage. In recent years, significant progresses have been made in synthesizing new MOFs with record high surface areas and pore volumes exceeding 7000 $m^2\ g^{-1}$ and 4 cc g^{-1} by utilizing longer organic linkers and activation with supercritical carbon dioxide (SCD).[29] To make use of the extremely high pore volumes and surface areas, porous MOFs are very promising candidate materials for high pressure gas storage. Studies have shown that the high pressure gravimetric gas storage capacities are basically proportional to their pore volumes or surface areas;[30−32] this means that the larger the porosity, the larger the gravimetric gas uptake by MOF materials under high pressure. To illustrate this effect of high porosity, we will provide some examples of such porous MOFs with high surface areas exhibiting the corresponding high gravimetric hydrogen, methane, and carbon dioxide storage capacities.

The high pressure gravimetric gas storage capacities are basically proportional to their pore volumes or surface areas; this means that the larger the porosity, the larger the gravimetric gas uptake under high pressure.

Hexacarboxylates have been widely employed to construct porous *rht*-type frameworks with high porosities. In this series of MOFs, the surface areas and pore volumes can be progressively boosted accordingly by increasing the length of the organic linkers. Notable examples include **NOTT-112**, **PCN-68/NOTT-116**, **PCN-69/NOTT-119**, **NU-100/PCN-610**, and **NU-111**.[2] The use of *rht*-type topology can effectively avoid framework interpenetration to create high pore volumes and BET surface areas, which are obviously favorable to high-pressure gas storage. For example, Schröder and co-workers utilized an elongated hexacarboxylate ligand with $Cu(NO_3)_2{\cdot}3H_2O$ to yield a *rht*-based MOF **NOTT-112** (Figure 1a).[33] The fully evacuated sample shows a high BET surface area of 3800 $m^2\ g^{-1}$ as well as excellent gravimetric H_2 adsorption capacities of 10.0 wt % at 77 bar and 77 K (Figure 1b). By using triple bond spacers to replace the phenyl spacers of the organic linker in **NOTT-112**, Hupp et al. synthesized a new MOF termed **NU-111**[34] with a high BET surface area of 4930 $m^2\ g^{-1}$. Owing to its higher surface area and pore volume, the total H_2 gravimetric uptake by **NU-111** reaches up to 13.5 wt % at similar conditions (Figure 1d), which is much higher than that of **NOTT-112**. As the size of organic linker is further elongated in **NU-110** (also termed **PCN-610**),[35,36] the resulting framework exhibits the third highest surface area of 6143 $m^2\ g^{-1}$ under activation using the SCD method. Most importantly, this MOF represents the highest total H_2 gravimetric uptake of 16.4 wt % at 70 bar and 77 K among reported *rht*-based MOFs (Figure 1f). It is worth noting that the record total H_2 gravimetric uptake by existing MOFs so far was published by Yaghi and co-workers for **MOF-210** (17.6 wt % at 80 bar and 77 K) with ultrahigh BET surface area exceeding 6200 $m^2\ g^{-1}$.[37] From these results, it appears that the gravimetric H_2 storage capacities of porous MOFs at 77 K are indeed proportional to their pore volumes or surface areas. When an operating temperature is no lower than −40 °C, these values are still short of the DOE H_2 storage target of over 5.5 wt % in gravimetric capacity under a maximum storage pressure of 100 atm.[38] Therefore, further endeavors should be focused on increasing the interactions of hydrogen gas molecules with MOFs to meet the DOE H_2 storage target.

The gravimetric CH_4 storage capacities of MOF materials under high pressure and room temperature (RT) are also basically dependent on their BET surface areas or pore volumes. To study the effect of porosities on gravimetric CH_4 methane storage at RT and 35 bar, He et al. examined a series of copper−tetracarboxylate frameworks (**NOTT-100**, **NOTT-101**, **NOTT-102**, **NOTT-103**, and **NOTT-109**) with similar structures whose porosities are systematically varied.[30] The results showed that the gravimetric methane uptake in this series of MOFs progressively increases with increasing porosity. Similarly, studies on a number

dx.doi.org/10.1021/jz501586e | J. Phys. Chem. Lett. 2014, 5, 3468−3479

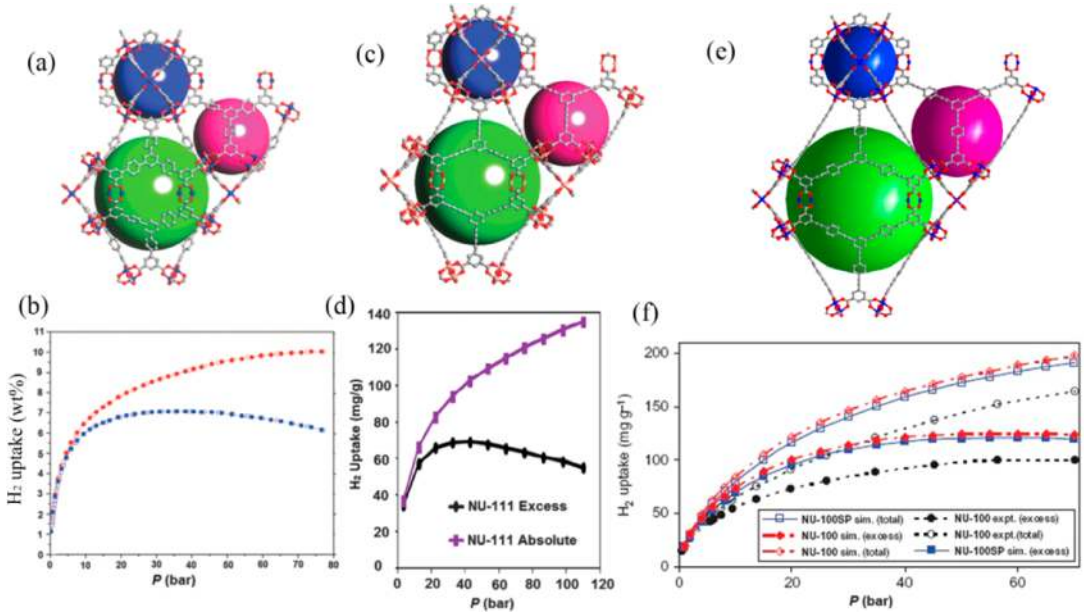

Figure 1. Different cages in the crystal structures of (a) **NOTT-112**, (c) **NU-111**, and (e) **NU-100**, and high pressure H_2 adsorption isotherms at 77 K for (b) **NOTT-112**, (d) **NU-111**, and (f) **NU-100** (black curves with open and closed symbols represent the total and excess gravimetric H_2 uptake, respectively). Reprinted with permission from refs 33 (Copyright 2009, Royal Society of Chemistry), 34 (Copyright 2012, American Chemical Society), and 35 (Copyright 2010, Nature Publishing Group).

of reported porous MOFs by Kong et al. revealed that the total gravimetric methane storage capacity at 60 bar and RT can be approximately calculated based on the following equation: C_{total} (cm^3 (STP) g^{-1}) = 147.2 + 0.06526 × BET (m^2 g^{-1}),[31] indicating that the larger the surface area, the larger the absolute CH_4 uptake by the MOF. Among existing MOFs, **MOF-210**[37] and **DUT-49**[39] have the maximum gravimetric methane uptakes of 536 and 540 cm^3 g^{-1}, respectively, at RT and 60 bar because of their extremely high BET surface areas of 6240 and 5476 m^2 g^{-1}. Simultaneously, by carefully examining the methane storage properties of six promising MOFs, Peng et al. also realized that values for the total gravimetric CH_4 uptake of the MOFs essentially linearly with surface area and can be approximately calculated based on the equation: C_{total} (cm^3 (STP) g^{-1}) = 127.1 + 0.07951 × BET (m^2 g^{-1}).[32] From this linear dependence, they estimate that a hypothetical MOF with surface area 7500 m^2/g and pore volume 3.2 cc/g could reach the current DOE gravimetric target of 0.5 g/g.[40]

The influence of framework porosities on gravimetric CO_2 capture has also been studied. Apparently, the total gravimetric CO_2 capture capacities of the MOFs at high pressure trend to increase as their BET surface areas increases. This trend can clearly explain the behavior of **DUT-49**: with extremely high BET surface area and pore volume (2.91 cm^3 g^{-1}), this MOF shows the highest total gravimetric CO_2 uptake of 947 cm^3 g^{-1} at RT and 30 bar.[38] Additionally, at RT and 50 bar, **MOF-210** represents the highest total gravimetric CO_2 uptake of about 2870 mg g^{-1}.[37]

Porous MOFs with Tunable Framework Structures and Porosities for Gas Storage and Separation. As demonstrated above, the main factor for the gravimetric gas storage capacities is still the porosity, which is related to the pore volume or BET surface area. For practical applications, the volumetric gas storage capacities might be even more important than gravimetric storage capacities given the fact that the vehicles will have limited space to put the tanks for gas storage. Apparently, high surface areas of MOFs cannot guarantee high volumetric gas storage capacities because such highly porous MOF materials tend to show low framework densities.[31] Ideal porous MOFs for high volumetric gas storage need to have balanced porosities and framework densities as well as high densities of suitable pore cages for the recognition of gas molecules.[30−32] By judicious selection of metal ions/clusters and bridging organic linkers, porous MOFs provide an ideal platform to tune their framework structures and thus densities, which enabled us to systematically optimize their gas storage capacities, particularly volumetric gas storage capacities.[41−44]

Ideal porous MOFs for high volumetric gas storage need to have balanced porosities and framework densities as well as high densities of suitable pore cages for the recognition of gas molecules.

The well-known MOF **HKUST-1**, first reported by Chui et al.,[41] has been widely investigated for high pressure methane storage. This 3D framework contains three different types of cages with small cages of ∼4, 10, and 11 Å in diameter for the recognition of methane molecules (Figure 2a). Although it has the moderate BET surface area of 1850 m^2 g^{-1} and low gravimetric CH_4 storage capacity of 0.216 g g^{-1}, this material exhibits an exceptionally high volumetric methane storage capacity of 267 cm^3 (STP) cm^{-3} at 298 K and 65 bar (Figure 2b), the highest reported so far.[32] This is the first MOF material with a volumetric methane storage capacity that meets the new DOE target if the packing density loss is ignored.[40] The window site of the small octahedral cage and open Cu^{2+} coordination site were found to be two of primary methane adsorption sites, as revealed

dx.doi.org/10.1021/jz501586e | J. Phys. Chem. Lett. 2014, 5, 3468−3479

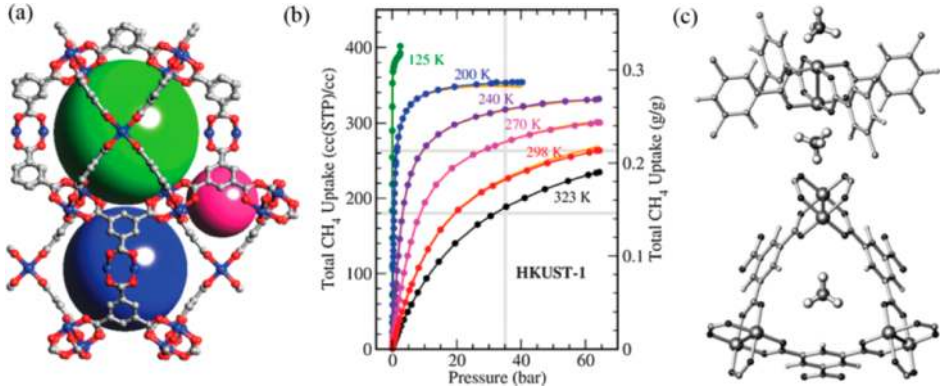

Figure 2. (a) Three different types of cages in **HKUST-1**. (b) Methane adsorption isotherms for **HKUST-1** at various temperatures. (c) Two primary adsorption sites for methane: open copper site (upper) and the small cage window site (down) in **HKUST-1**. Reprinted with permission from refs 32 (Copyright 2013, American Chemical Society) and 42 (Copyright 2010, Wiley-VCH).

by the high-resolution neutron powder diffraction experiments combined with a grand canonical Monte Carlo simulation (GCMC) (Figure 2c).[42] Therefore, the optimized structure and pore size within **HKUST-1** should be mainly responsible for its high volumetric methane storage capacity. Before this work, Chen and co-workers realized that the optimal pore spaces within **UTSA-20** have enabled the pore spaces to be fully utilized for methane storage, resulting in its very high volumetric methane storage of 195 cm^3 cm^{-3} at RT and 35 bar.[43]

To target high volumetric CO_2 uptake at RT and high pressure, MOF materials also need to have balanced porosities and framework densities to maximize the pore-usage efficiency. Hupp and co-workers developed a highly porous (3, 24)-connected MOF **NU-111** using a C_3-symmetrical organic linker, exhibiting a high surface area of 4930 m^2/g and pore volume of 2.09 cm^3/g.[34] Due to the balanced porosity and framework density, **NU-111** shows the highest absolute volumetric CO_2 uptake of 350 cm^3 cm^{-3} at RT and 30 bar. This value is higher than that of **MOF-210** (221 cm^3 cm^{-3}) and **NU-100** (250 cm^3 cm^{-3}) whose surface areas exceed 6000 m^2 g^{-1}.[31] Similarly, in terms of volumetric H_2 uptake, despite the lower BET surface area (2300 m^2 g^{-1}) and pore volume (1.08 cm^3 g^{-1}), **SNU-50**[45] exhibits higher absolute volumetric H_2 uptake of 50.0 g L^{-1} than 44 g L^{-1} in **MOF-210**[37] (the best one for gravimetric H_2 uptake) under similar conditions. It is reasonable to suggest that the optimum frameworks and pores/cage sizes within MOF materials play the most important part in optimizing the volumetric gas storage capacity rather than simply high BET surface areas and pore volumes.

The research efforts have been dedicated not only to the development of MOFs for gas storage applications but also to MOFs for gas separation, as well.[4,46−48] It is well established that rational control and tuning of small pore/window sizes within porous MOFs at the molecular level can efficiently improve their sieving effects for the selective separation of gas molecules. This is because their selective sorption behaviors are mainly determined by size-exclusive effects in which small gas molecules can go through the pore channels while large ones are blocked. Up to now, a large number of MOFs have shown the promising potential of the highly selective separation of gas mixtures by rationally and systematically tuning pore/window sizes.

Chen and co-workers designed and synthesized three 3D doubly interpenetrated primitive cubic MOFs, termed $Cu(FMA)(Pyz)_{0.5}$, $Cu(FMA)(4,4'\text{-Bipy})_{0.5}\cdot 0.25H_2O$, and $Cu(FMA)(4,4'\text{-Bpe})_{0.5}\cdot 0.5H_2O$ by self-assembly of fumarate (FMA) with different pillar linker pyrazine (Pyz), 4,4-bipyridine (4,4′-Bipy), and *trans*-bis-(4-pyridyl)ethylene (4,4′-Bpe).[49] Among these MOFs, the pore void spaces can be systematically tuned from nonporous condensed (Figure 3b) to a pore aperture of 1.4 × 1.8 Å (Figure 3d) and then 2.0 × 3.2 Å (Figure 3f), simply by increasing the pillar linker length. Sorption studies show that the dehydrated $Cu(FMA)(4,4'\text{-Bipy})_{0.5}$ does not take up both H_2 and N_2 at 77 K. Obviously, the small pore apertures of 1.4 × 1.8 Å within $Cu(FMA)(4,4'\text{-Bipy})_{0.5}$, which are much smaller than the sizes of H_2 (2.8 Å) and N_2 (3.64 Å) molecules, are believed to effectively block the entrance of gas molecules. In contrast, $Cu(FMA)(4,4'\text{-Bpe})_{0.5}$ with the rationally designed pore apertures of 2.0 × 3.2 Å shows selective sorption behavior with respect to different gas molecules. As shown in Figure 3i, this MOF can selectively absorb significant amount of H_2 (2.8 Å) while excluding Ar (3.4 Å), N_2 (3.64 Å), and CO (3.76 Å) at 77 K and 1 atm by taking advantage of size-exclusive effects. Furthermore, this framework also exhibits a certain degree of dynamics at a higher temperature of 195 K, in which the pore apertures can be enlarged to facilitate the entrance of some gas molecules, leading to the selective adsorption of CO_2 over CH_4 and N_2 at 195 K (Figure 3j).

Another promising example of systematically tuning pore sizes for the highly selective adsorption of CO_2 over N_2 and CH_4 was reported by Zaworotko and co-workers.[50] In this work, they constructed three different MOFs namely **SIFSIX-2-Cu**, **SIFSIX-2-Cu-i**, and **SIFSIX-3-Zn** using a rational crystal engineering or isoreticular chemistry strategy. The pore sizes in this series range from **SIFSIX-2-Cu** with pore dimensions of 13.05 Å × 13.05 Å, to doubly interpenetrated **SIFSIX-2-Cu-i** affording 5.15 Å × 5.15 Å pores, and finally to **SIFSIX-3-Zn** with 3.84 Å × 3.84 Å channels (Figure 4a). Despite the reduction in surface area compared with **SIFSIX-2-Cu**, the isostructural framework **SIFSIX-2-Cu-i** exhibits substantially higher CO_2 uptake of 121.2 cm^3 g^{-1} as well as 7−10 times higher CO_2/CH_4 and CO_2/N_2 IAST selectivities, as confirmed by column breakthrough tests. This remarkable increase was presumably attributable to the smaller pore size for **SIFSIX-2-Cu-i** than that of **SIFSIX-2-Cu**, resulting in the stronger interactions between the pore surfaces and guest CO_2 molecules. Most importantly, the IAST calculations combined with column breakthrough experiments further revealed that the framework of **SIFSIX-2-Zn**, with extremely narrow pore dimensions of 3.84 $Å^2$, shows the highest CO_2/CH_4 and CO_2/N_2 selectivities among this series of MOF materials (Figure 4b), indicating the best adsorption

dx.doi.org/10.1021/jz501586e | *J. Phys. Chem. Lett.* 2014, 5, 3468−3479

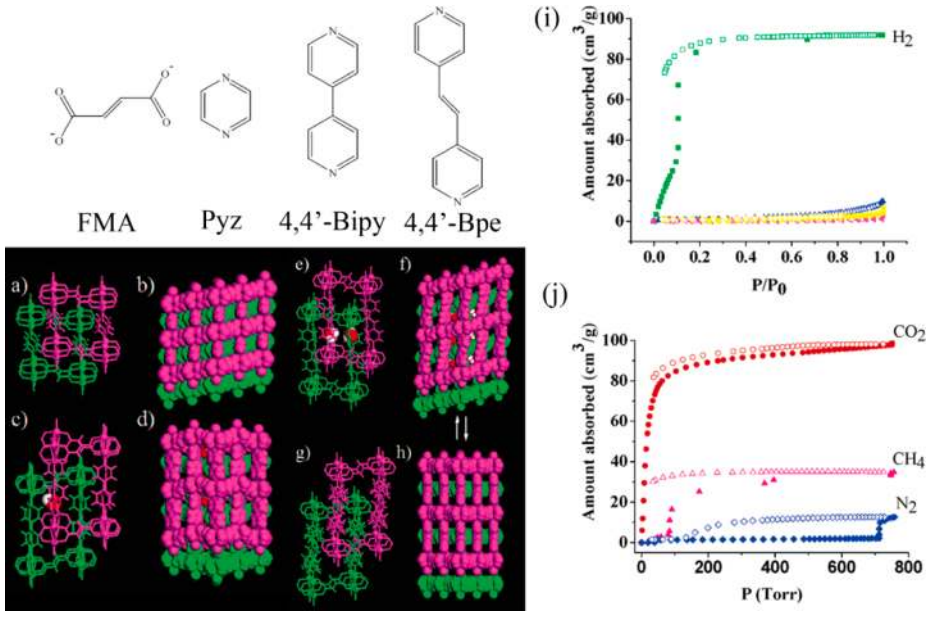

Figure 3. Crystal structures of frameworks $Cu(FMA)(Pyz)_{0.5}$ (a, b), $Cu(FMA)(4,4'\text{-Bipy})_{0.5}\cdot 0.25H_2O$ (c, d), $Cu(FMA)(4,4'\text{-Bpe})_{0.5}\cdot 0.5\ H_2O$ (e, f), and $Cu(FMA)(4,4'\text{-Bpe})_{0.5}$ (g, h) showing doubly interpenetrated primitive cubic nets and corresponding pore void spaces as well as gas sorption isotherms of $Cu(FMA)(4,4'\text{-Bpe})_{0.5}$ at (i) 77 K (H_2, green; N_2, blue; Ar, magenta; CO, yellow) and (j) 195 K (CO_2, red; CH_4, pink; N_2, blue). Reprinted with permission from ref 49 (Copyright 2007, American Chemical Society).

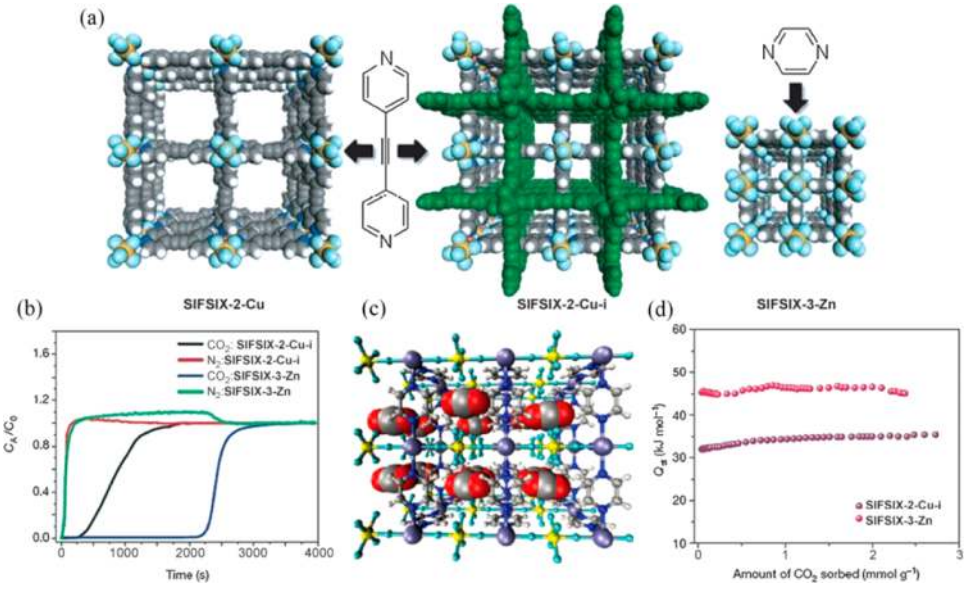

Figure 4. (a) The variable pore size channel structures of **SIFSIX-2-Cu**, **SIFSIX-2-Cu-i**, and **SIFSIX-3-Zn**. **SIFSIX-2-Cu**, pore size = 13.05 Å; **SIFSIX-2-Cu-i**, pore size = 5.15 Å; **SIFSIX-3-Zn**, pore size = 3.84 Å. (b) Breakthrough experiments on **SIFSIX-2-Cu-i** and **SIFSIX-3-Zn** with a 10:90 mixture of CO_2/N_2 (298 K, 1 bar). (c) The modeled structure of a 3 × 3 box of unit cells of **SIFSIX-3-Zn** reveals close interactions between the electropositive carbon atoms of CO_2 molecules and fluoride atoms of SIFSIX anions. (d) Q_{st} of CO_2 adsorption on **SIFSIX-2-Cu-i** and **SIFSIX-3-Zn** in the low-pressure region. Reprinted with permission from ref 50 (Copyright 2013, Nature).

selectivity toward CO_2 over N_2 or CH_4 observed until now. The isosteric heat of CO_2 adsorption (Q_{st}) in this series of MOFs progressively increased following **SIFSIX-2-Cu** (22 kJ mol^{-1}) < **SIFSIX-2-Cu-i** (31.9 kJ mol^{-1}) < **SIFSIX-2-Zn** (45 kJ mol^{-1}) (Figure 4d); this increase was believed to be a result of rationally tuning pore sizes in this series of MOFs, which can efficiently enhance the affinity of MOFs toward CO_2 molecules and, thus, the adsorptive selectivity of CO_2.

To tune pore size by framework interpenetration, Chen and co-workers have successfully achieved a micporous MOF, $Zn(BDC)(4,4'\text{-Bipy})_{0.5}$ (**MOF-508**) (BDC = 1,4-benzenedicarboxylate) for separation of aliphatic isomers.[51] This doubly interpenetrated MOF shows a reversible open−dense framework transformation, which is dependent on the uptake or removal of guest molecules. The open form of this MOF has 1D pores of 4.0 Å, which are slightly larger than the size of methane (3.8 Å). This feature allows its pore surface interactions with the linear parts of alkanes, making it potentially useful for the GC alkane separation. Apparently, the retention of alkanes on the column is mainly dependent on the length of the linear part

dx.doi.org/10.1021/jz501586e | J. Phys. Chem. Lett. 2014, 5, 3468−3479

of the alkane because of their different van der Waals interactions with the microporous MOF walls. As a result, the pentane and hexane mixtures can be straightforwardly separated in a GC column packed with single crystals of **MOF-508** according to the length of the linear part. This is the first example of such porous MOFs capable of selectively separating of linear alkanes from branched alkanes.

Using porous mixed MOFs (M'MOFs) as adsorbents, Chen et al. highlighted the first example of microporous materials termed **M'MOFs-2** and **-3** for their highly selective separation of C_2H_2/C_2H_4.[52] Owing to the smaller micropores compared with **M'MOF-2**, **M'MOF-3** shows remarkably higher separation selectivity with respect to C_2H_2/C_2H_4 separation by making use of the size-exclusion effect. To further tune the micropore shapes and sizes within M'MOFs to maximize such size-exclusion effect, the same group designed and synthesized four other porous M'MOFs (**M'MOFs-4−7**), in which the pore shapes and sizes were systematically modulated by the change in both metalloligands and organic ligands.[53] On the basis of IAST and breakthrough data, the separation capacity of **M'MOF-2a−7a** trends to follow the order **M'MOF-3** > **M'MOF-4** > **M'MOF-6** > **M'MOF-2** > **M'MOF-5** > **M'MOF-7**. This appears that the fine-tuning of the micropores within this series of M'MOFs is very crucial and important to target their highly selective recognition and thus separation of C_2H_2/C_2H_4.

Porous MOFs with Rationally Immobilized Functional Sites and Pore Surfaces for Gas Storage and Separation. Incorporation of functional sites within porous MOFs is another promising strategy to enhance their gas storage and separation capacities.[54] Generally, the interactions between porous MOFs and gas molecules are typically van der Waals interactions, which can be improved by the limited small pores within MOFs. However, the enhancement by such small pores for their strong interactions is very limited. It is, thus, very important to immobilize some functional sites such as open metal sites (OMSs), Lewis basic/acidic sites and dynamic groups to serve as specific binding sites, which can induce the strong interactions with gas molecules. To utilize such strong interactions for the recognition of gas molecules, some porous MOF materials with high gas storage and separation capacities have been successfully targeted in recent years.

The incorporation of some functional sites such as open metal sites, Lewis basic/acidic sites, and dynamic groups within porous MOFs can introduce the specific interactions for the recognition of gas molecules and, thus, remarkably enhance their gas storage and separation capacities.

Because of the very explosive nature of acetylene, acetylene storage must be realized at room temperature and under pressure of 0.2 MPa in terms of safety concerns, so it is a great demand to immobilize specific binding sites into porous MOFs for the enhanced interactions with acetylene and, thus, high acetylene storage. Chen and co-workers first demonstrated that the immobilization of OMSs into porous MOFs can remarkably enhance acetylene uptake.[55,56] The results demonstrated that **HKUST-1** and **MOF-505** with open Cu^{2+} sites take up a significantly larger amount of acetylene than others without the OMSs (Figure 5g). The strong binding of the open Cu^{2+} sites for acetylene molecules has been exclusively established by neutron powder diffraction studies on the fully deuterated acetylene loaded **HKUST-1** (Figure 5h). To further understand the effect of the OMSs on acetylene storage, the same group reported a series of isostructural MOFs $\mathbf{M_2(DHTP)}$ (M = Co^{2+}, Mn^{2+}, Mg^{2+}, and Zn^{2+}; DHTP = 2,5-dihydroxyterephthalate) with high density of different OMSs.[56] The OMSs within this series of isostructural MOFs exhibit differential interactions with acetylene molecule in which Co^{2+} has the strongest interactions with acetylene and a very high adsorption enthalpy of 50.1 kJ mol^{-1} at the low coverage. Such high adsorption enthalpies in $\mathbf{Co_2(DHTP)}$ leads to the highest volumetric acetylene storage capacity ever reported with a capacity of 230 cm^3 cm^{-3} (STP) at 295 K and 1 atm (Figure 5i). The high-resolution neutron powder diffraction studies on acetylene-loaded $\mathbf{Co_2(DHTP)}$ suggest that the open Co^{2+} sites have very strong interactions with acetylene molecules to exhibit a Co−C bonding distance of 2.65 Å (Figure 5j). Such strong interactions of open Co^{2+} sites with acetylene was considered to be the main reason for the extraordinarily high acetylene storage capacity of $\mathbf{Co_2(DHTP)}$, which was also exclusively confirmed by the first-principles calculations.

The effect of OMSs on the H_2 adsorption at low pressure has been realized by Chen et al. in 2005.[57] In this study, they first utilized a tetracarboxylic linker containing *meta*-benzenedicarboxylate units to construct a *NbO* type framework **MOF-505** (also termed **NOTT-100**[58]). By removal of the coordinated water molecules, open Cu^{2+} sites can be simply introduced into pore surface to enhance the hydrogen−framework interactions and, thus, the H_2 uptake at 77 K and 1 bar. By taking advantage of neutron diffraction experiments and theoretical calculations, Zhou and co-workers also demonstrated that the created OMSs within a series of $\mathbf{M_2(DHTP)}$ materials are the primary and strongest H_2 binding sites, which can significantly increase the H_2 uptake by the M^{2+}−H_2 interactions.[59]

The separations of light hydrocarbons into single components are very important industrial processes because all of them are very important energy resources or raw chemicals in the petrochemical industry. To systematically investigate the potential of MOF materials for hydrocarbons separation, He et al. carefully selected a total of 19 different MOFs in a wide range of functionalities.[60] In all separation tasks investigated, it was found that MOFs with high density of OMSs, such as **Co-MOF-74**, **Mg-MOF-74**, and **Fe-MOF-74**, have significantly better separation performance than other MOFs. In particular, **Fe-MOF-74** suggests the most potential to "fractionate" a 6-component $CH_4/C_2H_2/C_2H_4/C_2H_6/C_3H_6/C_3H_8$ mixture to yield individual pure components. By making use of neutron powder diffraction experiments combined with computational modeling, Long and co-workers demonstrated that the unsaturated hydrocarbons acetylene, ethylene, and propylene in **Fe-MOF-74** displayed side−on binding modes with Fe−C distances in the range of 2.42 to 2.60 Å, whereas the interactions of both ethane and propane with the Fe^{2+} cations are weaker due to the elongated Fe−C distance of approximately 3 Å (Figure 6a).[61] As a result of such different metal−adsorbate interactions, this material displays an initial steep rise in the unsaturated hydrocarbons acetylene, ethylene, and propylene isotherms with a correspondingly slow increase in the propane and ethane isotherms (Figure 6b), suggesting a

dx.doi.org/10.1021/jz501586e | J. Phys. Chem. Lett. 2014, 5, 3468−3479

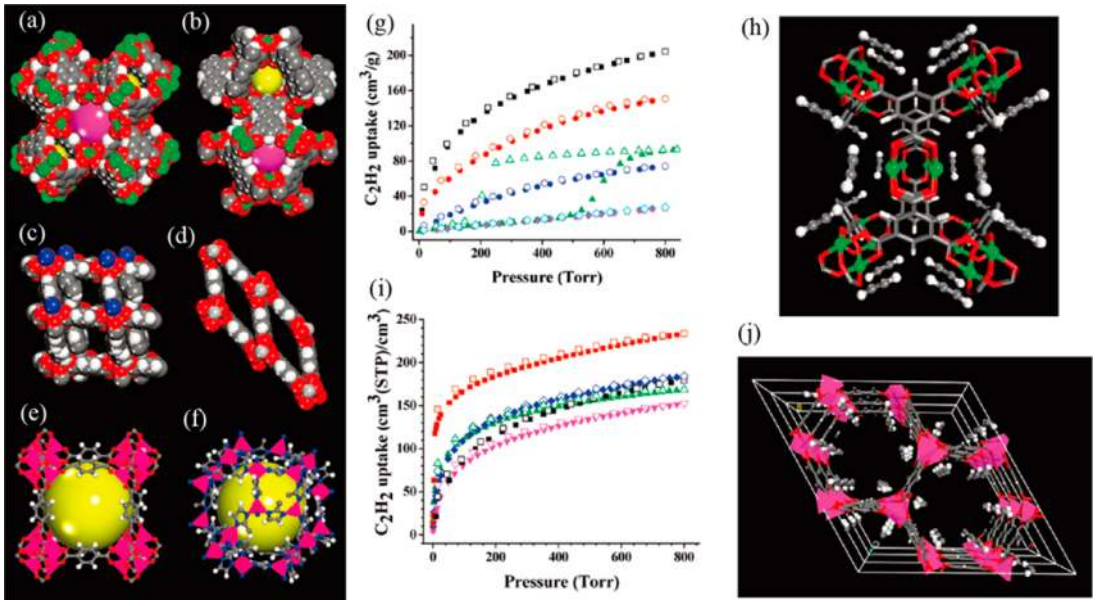

Figure 5. Single-crystal X-ray structures of (a) **HKUST-1**, (b) **MOF-505**, (c) **MOF-508**, (d) **MIL-53**, (e) **MOF-5**, and (f) **ZIF-8**, showing open Cu^{2+} sites (green), 3D frameworks, and corresponding pore/cage sizes. (g) Acetylene adsorption isotherms of microporous MOFs at 295 K; **HKUST-1** (black); **MOF-505** (red); **MOF-508** (green); **MIL-53** (blue); **MOF-5** (cyan); and **ZIF-8** (pink). (h) The crystal structure of one C_2D_2 per Cu-loaded **HKUST-1**, showing the open Cu^{2+} sites for the recognition of acetylene molecules. (i) Acetylene adsorption isotherms of porous MOFs at 295 K (**Co_2(DHTP)** (red); **Mn_2(DHTP)** (blue); **Mg_2(DHTP)** (green); **HKUST-1** (black); **Zn_2(DHTP)** (pink). (j) The crystal structure of 0.54 C_2D_2 per Co-loaded **Co_2(DHTP)** along the *c* axis exhibiting the high density of adsorbed acetylene molecules in pseudo-one-dimensional arrays. Reprinted with permission from refs 55 (Copyright 2009, American Chemical Society) and 56 (Copyright 2010, Wiley-VCH).

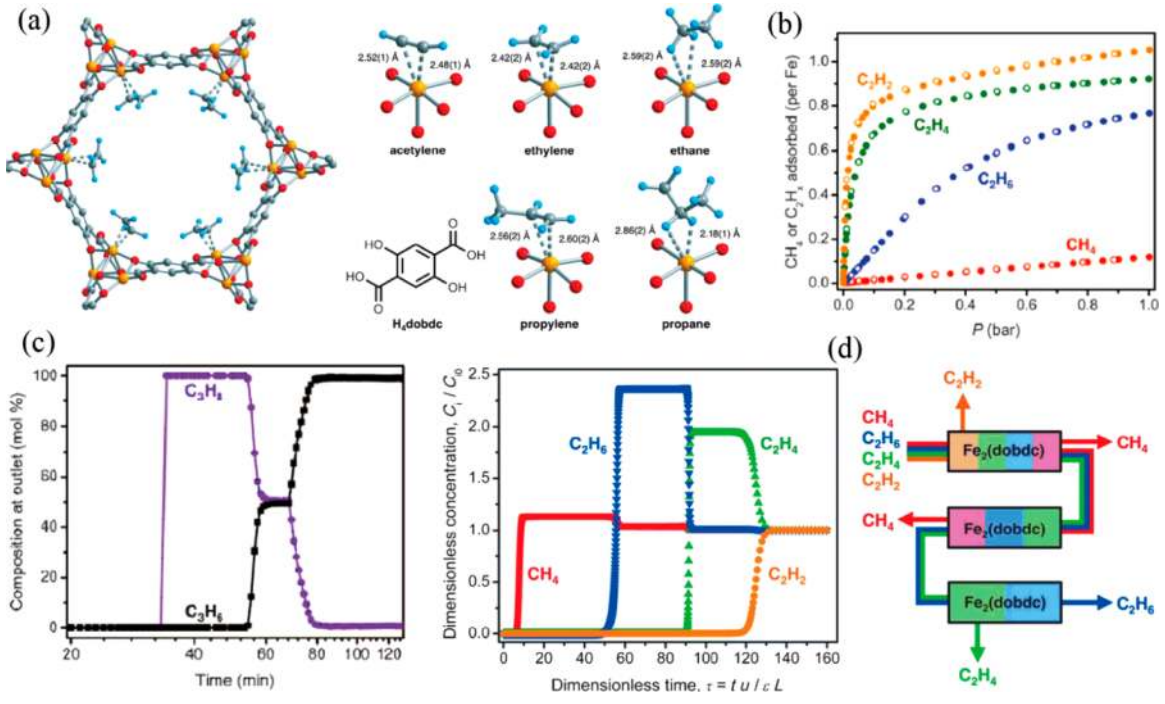

Figure 6. (a) Left: A portion of the solid-state structure of Fe_2(dobdc)·$2C_2D_4$; orange, red, gray, and blue spheres represent Fe, O, C, and D atoms, respectively. Right: the H_4(dobdc) ligand and the first coordination spheres for the iron centers in the solid-state structures obtained upon dosing **Fe-MOF-74** with acetylene, ethylene, ethane, propylene, and propane. (b) Gas adsorption isotherms for methane, ethane, ethylene, and acetylene. (c) Experimental breakthrough curves for the adsorption of equimolar propane/propylene mixtures flowing through a 1.5 mL bed of **Fe-MOF-74** at 318 K with a total gas flow of 2 mL/min at atmospheric pressure. (d) Left: Calculated methane (red), ethane (blue), ethylene (green), and acetylene (orange) breakthrough curves for an equimolar mixture of the gases at 1 bar flowing through a fixed bed of **Fe-MOF-74** at 318 K. Right: Schematic representation of the separation of a mixture of methane, ethane, ethylene, and acetylene by using just three packed beds of **Fe-MOF-74** in a vacuum-swing adsorption or temperature-swing adsorption process. Reprinted with permission from ref 61 (Copyright 2012, Science).

dx.doi.org/10.1021/jz501586e | *J. Phys. Chem. Lett.* 2014, 5, 3468−3479

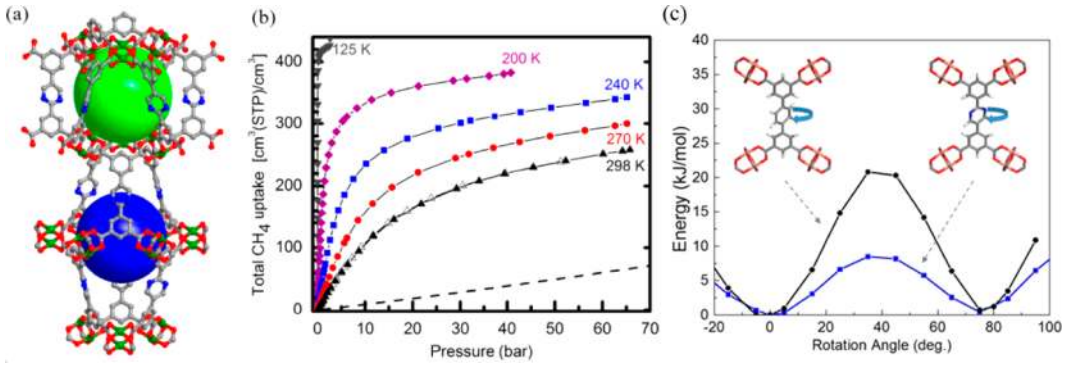

Figure 7. (a) X-ray crystal structure of **UTSA-76**. (b) Temperature dependent high-pressure methane sorption isotherms of **UTSA-76** (data of pure methane gas stored in a high pressure gas tank is represented as dash black curve). (c) The variation of the total energy as the central rings of the **UTSA-76** and **NOTT-101** linker are rotated around the linker backbone, derived from DFT calculations. Reprinted with permission from ref 62 (Copyright 2014, American Chemical Society).

promising potential for use in small hydrocarbon separations. Breakthrough data indicated that **Fe-MOF-74** can efficiently separate an equimolar mixture of ethylene and ethane into the pure component gases from 99 to 99.5% purity. For an equimolar mixture of propylene/propane gas, 100% pure propane can be obtained from the outlet gas, and greater than 99% propylene are produced during the desorption step (Figure 6c). When four-component methane/ethane/ethylene/acetylene mixtures go through the three packed beds of **Fe-MOF-74**, it might be possible to procure pure methane, ethane, ethylene, and acetylene in a different process (Figure 6d). Thus, their results highlighted the extraordinary prospects for the usage of **Fe-MOF-74** as a solid adsorbent in the separation of small hydrocarbons.

To immobilize dynamic pyrimidine groups into a porous MOF, our recent work highlighted a novel material **UTSA-76** exhibiting record high methane storage working capacity.[62] The framework in **UTSA-76** has exactly same structure and comparable porosity with **NOTT-101** (Figure 7a). However, the volumetric methane storage capacity was significantly improved from 237 cm^3 (STP) cm^{-3} in **NOTT-101** to 257 cm^3 (STP) cm^{-3} in **UTSA-76** at 65 bar and 298 K (Figure 7b). It is also notable that **UTSA-76** shows a record methane storage working capacity of ~200 cm^3 (STP) cm^{-3}, featuring it as a very promising material for methane/natural gas storage for transport applications. The computational studies and neutron scattering experiments suggest that the exceptionally high working capacity in **UTSA-76** was probably attributed to the central "dynamic" pyrimidine groups within **UTSA-76** (Figure 7c), which was believed to be capable of adjusting their orientations to optimize the methane packing at high pressure.

In recent years, MOFs have attracted great attention as porous materials for CO_2 capture and separation. The incorporation of functional sites within porous MOFs has been shown to be a powerful strategy that can significantly improve their post-combustion CO_2 capture and separation capacities.[3,63−67] In this regard, Chen and co-workers systematically examined a series of porous MOFs that have different pore structures, surface areas, and pore-surface functionalities for their performance on post-combustion CO_2 capture.[65] The results indicated that the immobilization of specific sites such as open metal sites and $-NH_2$ sites can certainly induce their strong interactions with CO_2 molecules and then enhance the capacity of CO_2 capture and separation. Notably, **Mg-MOF-74** with extremely high density of open Mg^{2+} sites represents the highest gravimetric and

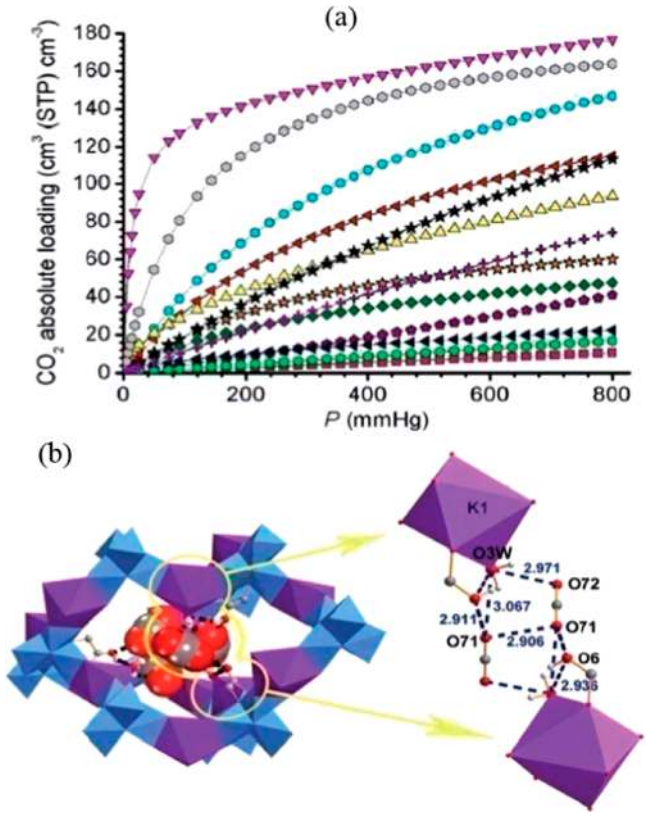

Figure 8. (a) Comparison of the absolute loading of CO_2 at 296 K on **UTSA-16** and some selected MOFs. From top to bottom, **Mg-MOF-74** (magenta down triangle), **UTSA-16** (gray hexagon), **Zn-MOF-74** (cyan circle), **bio-MOF-11** (red left triangle), Cubtc (black star), Cu-tdpat (yellow up triangle), **UTSA-20** (violet cross), **ZIF-78** (orange star), $Zn_5(bta)_6(tda)_2$ (olive diamond), Zn(bdc)(dabco) (purple pentagon), **MIL-101** (navy left triangle), Yb(bpt) (green hexagon) and **MOF-177** (pink square). (b) CO_2 dimers trapped within the cage, and the cooperative interactions between trapped CO_2 molecules with the framework. Reprinted with permission from ref 65 (Copyright 2012, Nature Publishing Group).

volumetric adsorption capacity on MOFs at 0.1 bar so far.[66] Furthermore, they also discovered a MOF $[K(H_2O)_2Co_3(cit)(Hcit)]$ (**UTSA-16**) (H_4cit = citric acid) exhibiting extraordinarily high volumetric uptake of CO_2 (up to 160 cm^3 cm^{-3}) at ambient conditions (Figure 8a). In CO_2(50%)/CH_4(50%) and CO_2(15%)/N_2(85%) flue gas mixture, simulated breakthrough

dx.doi.org/10.1021/jz501586e | J. Phys. Chem. Lett. 2014, 5, 3468−3479

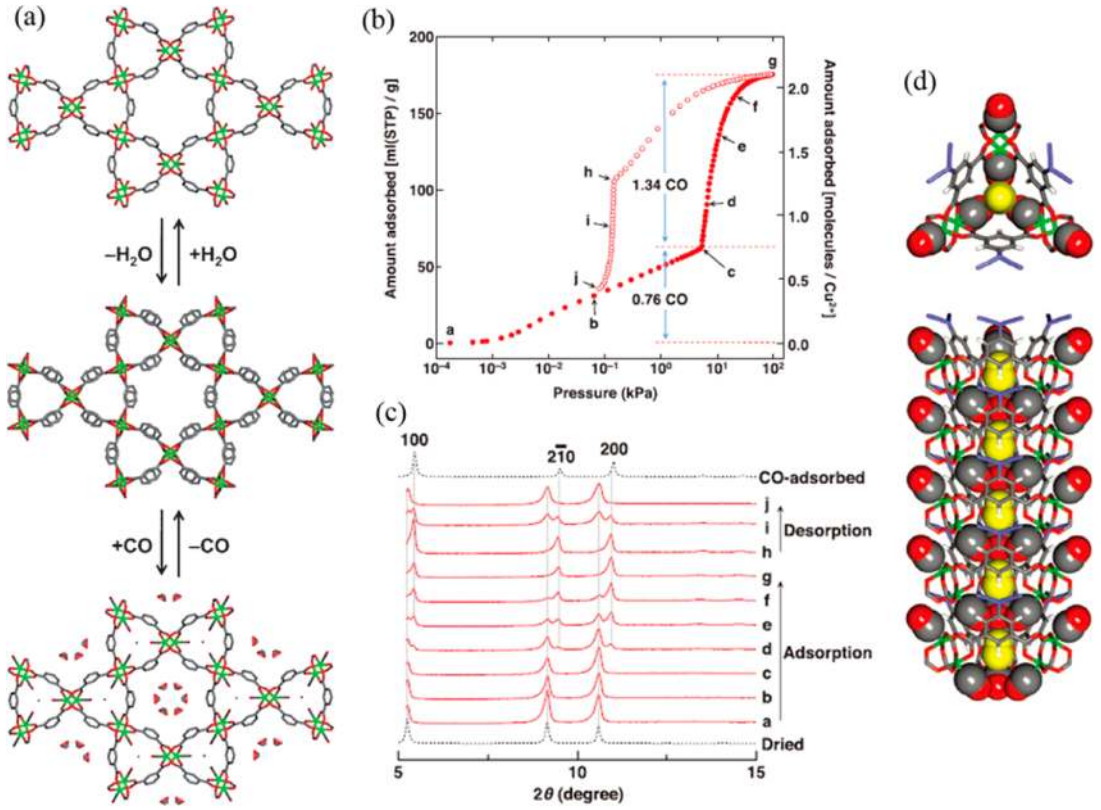

Figure 9. (a) Reversible structural transformation of the channels between **PCP 1** (upper), **PCP 2** (middle), and **PCP 3** (down). (b) CO sorption isotherms at 120 K. Filled and open symbols represent adsorption and desorption data, respectively. (c) XRPD patterns measured at each point (a to j) shown in the CO sorption isotherms. The simulated patterns for the dried **PCP 2** and CO-adsorbed **PCP 3** are shown at the bottom and top, respectively. (d) X-ray crystal structures of CO-adsorbed **PCP 3**: top (upper) and side (down) views of CO adsorbed channel S. Reprinted with permission from ref 69 (Copyright 2013, Science).

experiments indicated that **UTSA-16** shows a high separation selectivity and capacity for CO_2 capture applications at ambient conditions. Both the immobilized terminal water molecules and suitable pore/cage space are considered to be responsible for its high CO_2 separation selectivity and capacity because of the strong interactions between pore surfaces with CO_2 molecules, as revealed by neutron diffraction studies (Figure 8b). Additionally, Long and co-workers also demonstrated that the alkylamino-functionalization within porous MOFs obtained though post-synthetic modification can improve the selective adsorption of CO_2 over CH_4 and N_2 at low pressure.[67] Very recently, by incorporation of functional bulky hydrophobic links, Yaghi and co-workers reported three hydrophobic MOF materials, namely **ZIF-300**, **ZIF-301**, and **ZIF-302**.[68] All three MOFs are capable of effective separation of CO_2 from N_2 even under humid conditions without any loss of performance over three cycles and can be readily regenerated by using a N_2 flow at ambient temperature, making them very promising for the use in practical applications.

Using a soft nanoporous MOF material with open metal sites, Kitagawa and co-workers have achieved unprecedented highly effective trapping of CO from a gas mixture with N_2.[69] Self-assembly of paddle-wheel clusters $Cu_2(CO_2)_4$ with 5-azidoisophthalate (aip) leads to an infinite kagomé-type 2D framework $[Cu(aip)(H_2O)](solvent)_n$ (**PCP 1**) (aip = 5-azidoisophthalate). After removal of the coordinated water molecules, the 2D structure of **PCP 1** can be reversibly transformed into **PCP 2**, which has a 3D framework by forming the paddle-wheel chains along the *c* axis (Figure 9a). The activated **PCP 2** can preferentially take up much more amount of CO (175 mL (STP) g^{-1}) over that of N_2 (71 mL (STP) g^{-1}) at 80 kPa with distinct two-step adsorption (Figure 9b). During the second CO adsorption step after point c, a structural transformation occurs on **PCP 2** to form the resulting **PCP 3** that has a similar structure to that of **PCP 1**, leading to a steeply increased CO uptake (Figure 9c). The coordination of CO molecules toward open Cu^{2+} ions to form a Cu^{2+}−CO bond was considered to be the main reason that induces such structure transformation from **PCP 2** to **PCP 3**, which is more favorable to further accommodation of CO molecules in the center of open channels. Most importantly, **PCP 2** exhibits the unprecedented high separation ability in a wide range of CO mixtures with N_2. The coordination of CO molecules with open Cu^{2+} ions combined with 1D small channels of **PCP 2** with an open-close system were proposed to be capable of enhancing the selectivity of CO over N_2. Their work opens a promising new route to introduce open Cu^{2+} ions into a soft nanoporous material for the high separation selectivity of CO from mixtures with N_2.

MOF materials can also be widely fabricated into thin membranes for their gas separation. The use of functional linkers is a promising strategy to introduce gas selectivity in a MOF membrane. Using a stepwise deposition method, two pillared layered MOF $Cu_2(ndc)_2(dabco)$ (ndc = 1,4-naphtalenedicarboxylate; dabco = 1,4-diazabicyclo(2.2.2)octane) and $Cu_2(BME\text{-}bdc)_2(dabco)$ (BME-bdc = 2,5-bis(2-methoxyethoxy)-1,4-benzenedicarboxylate) were selected by Fischer and co-workers to fabricate into MOF membranes for gas separation.[70] $Cu_2(ndc)_2(dabco)$ is

dx.doi.org/10.1021/jz501586e | J. Phys. Chem. Lett. 2014, 5, 3468−3479

a large-pore MOF in which there are no specific interactions between the pore surface and gas molecules. Thus, Knudsen separation factors (0.6) were observed in the CO_2/CH_4 separation. In contrast, $Cu_2(BME\text{-}bdc)_2(dabco)$ included a linker BME-bdc with two long ether side functional groups ($O(CH_2)_2OCH_3$). This polar functionalization was expected to increase the framework affinity for CO_2 compared to CH_4. As a result, the $Cu_2(BME\text{-}bdc)_2(dabco)$ membrane in equimolar mixtures of CO_2/CH_4 exhibits high adsorption selectivity of CO_2 over CH_4 with a selectivity factor of 4.5, which is great higher than the corresponding Knudsen coefficient (0.6). Such high selectivity of CO_2 over CH_4 in $Cu_2(BME\text{-}bdc)_2(dabco)$ membrane was mainly attributed to the preferential interactions between CO_2 and the framework rather than molecular sieving effect. This study demonstrated the concept of introducing functional groups into porous MOFs to remarkably improve the separation efficiency of MOF membranes.

Conclusions and Perspective. In this Perspective, we have outlined three types of successful strategies, including high porosities, optimum framework structures and porosities, and immobilized functional sites, to construct porous MOFs for their promising potential on gas storage and separation. From the reviewed literatures, we have identified that the gravimetric gas storage capacities of porous MOFs are basically proportional to their pore volumes or surface areas under high pressure. A large number of MOFs with extremely high porosities exceeding 6000 m^2/g have been studied and reported, exhibiting corresponding high gravimetric H_2, CH_4, or CO_2 storage capacities. As demonstrated computationally by Hupp et al., the hypothetical maximum surface area for a MOF material can be up to ~14600 m^2/g; thus, it is expected that the new record gravimetric gas storage capacities will be probably targeted as the BET surface areas will be further increased in the near future. Compared with the gravimetric gas storage capacity, a high volumetric gas storage capacity is the most critical metric for practical H_2/CH_4 fueling in vehicles. In order to target the high volumetric gas uptake capacity, the optimum framework structures and pore/cage sizes need to be well studied and explored rather than simply pursuing ultrahigh porosity. The ability to rationally and systematically tune the pore or window size has enabled us to further explore the very promising MOF materials for small gas separation and purification. By immobilizing different functional sites within porous MOFs to serve as specific binding sites for the recognition of gas molecules, it is certainly capable of enhancing their gas storage and separation capacities, particularly at moderate temperatures. Open metal sites within porous MOFs play much more important roles for their gas storage under low pressure. Because it is not practical to release all the gas molecules under vacuum and it is necessary to have certain pressures within the tanks filled with MOF materials to facilitate the fast release of the gas molecules (for example, 5 bar is widely accepted as the releasing pressure for methane storage), MOFs with high densities of open metal sites are not necessarily favorable to the overall high gas storage working capacities, which have been clearly demonstrated in MOF-74 series for their methane storage.[71] With increased understanding of the relationship between MOFs' porosity/structure/functionalization and their gas storage/separation properties, it is expected that some even better MOF materials for gas storage and separation will be rationally designed and targeted in the near future.

AUTHOR INFORMATION

Corresponding Author

* E-mail: banglin.chen@utsa.edu.

Notes

The authors declare no competing financial interest.

Biographies

Bin Li obtained his Ph.D. in 2012 from the Fujian Institute of Research on the Structure of Matter, Chinese Academy of Sciences, under the supervision of Prof. Zhong-Ning Chen. After obtaining his Ph.D. degree, he joined the group of Prof. Banglin Chen as a postdoctoral fellow. His current research interest focuses on multifunctional metal−organic frameworks.

Hui-Min Wen earned her Ph.D. in 2010 from Fujian Institute of Research on the Structure of Matter, Chinese Academy of Sciences, under the supervision of Prof. Cheng-Neng Chen and Prof. Zhong-Ning Chen. She joined Prof. Cheng-Neng Chen's Group as an assistant research scientist during 2010−2013, and she was promoted to associate researcher in 2014. Now, she is working with Prof. Banglin Chen as a postdoctoral fellow, focusing on design and synthesis of multifunctional metal−organic frameworks.

Wei Zhou received his Ph.D. in 2005 from the University of Pennsylvania, under the supervision of Prof. John E. Fischer. From 2005 to 2007, he was a postdoctoral researcher at the NIST Center for Neutron Research (NCNR), working with Dr. Taner Yildirim. After that, he was appointed to his current position as a research scientist at NCNR and the University of Maryland. His research interests are in the areas of novel porous materials, computational materials design, and neutron spectroscopy.

Banglin Chen received B.S. (1985) and M.S. (1988) degrees in Chemistry from Zhejiang University in China and his Ph.D. from National University of Singapore in 2000. He has been working with Professors Omar M. Yaghi at University of Michigan, Stephen Lee at Cornell University, and Andrew W. Maverick at Louisiana State University as the postdoctoral fellow during 2000−2003 before joining the University of Texas-Pan American in 2003. He moved to the University of Texas at San Antonio in August 2009, and now, he is a Professor of Chemistry. See more details at http://www.utsa.edu/chem/chen.html.

ACKNOWLEDGMENTS

This work was supported by grant AX-1730 from the Welch Foundation (B.C.).

REFERENCES

(1) Furukawa, H.; Cordova, K. E.; O'Keeffe, M.; Yaghi, O. M. The Chemistry and Applications of Metal−Organic Frameworks. *Science* **2013**, *341*, 6149−6160.

(2) He, Y.; Li, B.; O'Keeffe, M.; Chen, B. Multifunctional Metal−Organic Frameworks Constructed from Meta-Benzenedicarboxylate units. *Chem. Soc. Rev.* **2014**, *43*, 5618−5656.

(3) Sumida, K.; Rogow, D. L.; Mason, J. A.; McDonald, T. M.; Bloch, E. D.; Herm, Z. R.; Bae, T.-H.; Long, J. R. Carbon Dioxide Capture in Metal−Organic Frameworks. *Chem. Rev.* **2012**, *112*, 724−781.

(4) Li, J.-R.; Sculley, J.; Zhou, H.-C. Metal−Organic Frameworks for Separations. *Chem. Rev.* **2012**, *112*, 869−932.

(5) Cui, Y.; Yue, Y.; Qian, G.; Chen, B. Luminescent Functional Metal−Organic Frameworks. *Chem. Rev.* **2012**, *112*, 1126−1162.

(6) Yoon, M.; Srirambalaji, R.; Kim, K. Homochiral Metal−Organic Frameworks for Asymmetric Heterogeneous Catalysis. *Chem. Rev.* **2012**, *112*, 1196−231.

(7) Horcajada, P.; Gref, R.; Baati, T.; Allan, P. K.; Maurin, G.; Couvreur, P.; Férey, G.; Morris, R. E.; Serre, C. Metal−Organic Frameworks in Biomedicine. *Chem. Rev.* **2012**, *112*, 1232−1168.

(8) Wang, C.; Zhang, T.; Lin, W. Rational Synthesis of Noncentrosymmetric Metal−Organic Frameworks for Second-Order Nonlinear Optics. *Chem. Rev.* **2012**, *112*, 1084−1104.

(9) Yu, J.; Cui, Y.; Xu, H.; Yang, Yu.; Wang, Z.; Chen, B.; Qian, G. Confinement of Pyridinium Hemicyanine Dye within an Anionic Metal−Organic Framework for Two-Photon-Pumped Lasing. *Nat. Commun.* **2013**, *4*, 2719−2725.
(10) Batten, S. R.; Robson, R. Interpenetrating Nets: Ordered, Periodic Entanglement. *Angew. Chem., Int. Ed.* **1998**, *37*, 1460−1494.
(11) Carlucci, L.; Ciani, G.; Proserpio, D. M.; Sironi, A. 1-, 2-, and 3-Dimensional Polymeric Frames in the Coordination Chemistry of $AgBF_4$ with Pyrazine. The First Example of Three Interpenetrating 3-Dimensional Triconnected Nets. *J. Am. Chem. Soc.* **1995**, *117*, 4562−4569.
(12) Subramanian, S.; Zaworotko, M. J. Porous Solids by Design: $[Zn(4,4'\text{-bpy})_2(SiF_6)]_n \cdot x$DMF, a Single Framework Octahedral Coordination Polymer with Large Square Channels. *Angew. Chem., Int. Ed.* **1995**, *34*, 2127−2129.
(13) Allison, S. A.; Barrer, R. M. Sorption in the β-phases of Transition Metal(II) Tetra-(4-methylpyridine)thiocyanates and Related Compounds. *J. Chem. Soc. A* **1969**, 1717−1723.
(14) Kinoshita, Y.; Matsubara, I.; Higuchi, T.; Saito, Y. The Crystal Structure of Bis(adiponitrilo) Copper(I) Nitrate. *Bull. Chem. Soc. Jpn.* **1959**, *32*, 1221−1226.
(15) Corma, A.; Rey, F.; Rius, J.; Sabater, M. J.; Valencia, S. Supramolecular Self-Assembled Molecules as Organic Directing Agent for Synthesis of Zeolites. *Nature* **2004**, *431*, 287−290.
(16) Buser, H. J.; Schwarzenbach, D.; Petter, W.; Ludi, A. The Crystal Structure of Prussian Blue: $Fe_4[Fe(CN)_6]_3 \cdot xH_2O$. *Inorg. Chem.* **1977**, *11*, 2704−2710.
(17) Jiang, T.; Lough, A.; Ozin, G. A.; Bedard, R. L.; Broach, R. Synthesis and Structure of Microporous Layered Tin(IV) Sulfide Materials. *J. Mater. Chem.* **1998**, *8*, 721−732.
(18) Gardner, G. B.; Venkataraman, D.; Moore, J. S.; Lee, S. Spontaneous Assembly Of a Hinged Coordination Network. *Nature* **1995**, *374*, 792−795.
(19) Yaghi, O. M.; Li, G.; Li, H. Selective Binding and Removal of Guests in a Microporous Metal−Organic Framework. *Nature* **1995**, *378*, 703−706.
(20) Yaghi, O. M.; Li, H. Hydrothermal Synthesis of a Metal−Organic Framework Containing Large Rectangular Channels. *J. Am. Chem. Soc.* **1995**, *117*, 10401−10402.
(21) Venkataraman, D.; Gardner, G. B.; Lee, S.; Moore, J. S. Zeolite-like Behavior of a Coordination Network. *J. Am. Chem. Soc.* **1995**, *117*, 11600−11601.
(22) Yaghi, O. M.; Li, H.; Groy, T. L. Construction of Porous Solids from Hydrogen-Bonded Metal Complexes of 1,3,5-Benzenetricarboxylic Acid. *J. Am. Chem. Soc.* **1996**, *118*, 9096−9101.
(23) Kondo, M.; Yoshitomi, T.; Seki, K.; Matsuzaka, H.; Kitagawa, S. Three-Dimensional Framework with Channeling Cavities for Small Molecules: $\{[M_2(4,4'\text{-bpy})_3(NO_3)_4] \cdot xH_2O\}_n$ (M = Co, Ni, Zn). *Angew. Chem., Int. Ed. Engl.* **1997**, *36*, 1725−1727.
(24) Li, H.; Eddaoudi, M.; Groy, T. L.; Yaghi, O. M. Establishing Microporosity in Open Metal−Organic Frameworks: Gas Sorption Isotherms for Zn(BDC) (BDC = 1,4-Benzenedicarboxylate). *J. Am. Chem. Soc.* **1998**, *120*, 8571−8572.
(25) Li, H.; Eddaoudi, M.; O'Keeffe, M.; Yaghi, O. M. Design and Synthesis of an Exceptionally Stable and Highly Porous Metal−Organic Framework. *Nature* **1999**, *402*, 276−279.
(26) Kepert, C. J.; Rosseinsky, M. J. Zeolite-like Crystal Structure of an Empty Microporous Molecular Framework. *Chem. Commun.* **1999**, 375−376.
(27) Batten, S. R.; Champness, N. R.; Chen, X.-M.; Garcia-Martinez, J.; Kitagawa, S.; Öhrström, L.; O'Keeffe, M.; Suh, M. P.; Reedijk, J. Coordination Polymers, Metal−Organic Frameworks and the Need for Terminology Guidelines. *CrystEngComm* **2012**, *14*, 3001−3004.
(28) Chen, B.; Eddaoudi, M.; Hyde, S. T.; O'Keeffe, M.; Yaghi, O. M. Interwoven Metal−Organic Framework on a Periodic Minimal Surface with Extra-Large Pores. *Science* **2001**, *291*, 1021−1023.
(29) Farha, O. K.; Eryazici, I.; Jeong, N. C.; Hauser, B. G.; Wilmer, C. E.; Sarjeant, A. A.; Snurr, R. Q.; Nguyen, S. T.; Yazaydın, A. Ö.; Hupp, J. T. Metal−Organic Framework Materials with Ultrahigh Surface Areas: Is the Sky the Limit? *J. Am. Chem. Soc.* **2012**, *134*, 15016−15021.
(30) He, Y.; Zhou, W.; Yildirim, T.; Chen, B. A Series of Metal−Organic Frameworks with High Methane Uptake and an Empirical Equation for Predicting Methane Storage Capacity. *Energy Environ. Sci.* **2013**, *6*, 2735−2744.
(31) Kong, G.-Q.; Han, Z.-D.; He, Y.; Ou, S.; Zhou, W.; Yildirim, T.; Krishna, R.; Zou, C.; Chen, B.; Wu, C.-D. Expanded Organic Building Units for the Construction of Highly Porous Metal−Organic Frameworks. *Chem.−Eur. J.* **2013**, *19*, 14886−14894.
(32) Peng, Y.; Krungleviciute, V.; Eryazici, I.; Hupp, J. T.; Farha, O. K.; Yildirim, T. Methane Storage in Metal−Organic Frameworks: Current Records, Surprise Findings, and Challenges. *J. Am. Chem. Soc.* **2013**, *135*, 11887−11894.
(33) Yan, Y.; Lin, X.; Yang, S.; Blake, A. J.; Dailly, A.; Champness, N. R.; Hubberstey, P.; Schröder, M. Exceptionally High H_2 Storage by a Metal-OFarharO. K.ganic Polyhedral Framework. *Chem. Commun.* **2009**, 1025−1027.
(34) Farha, O. K.; Wilmer, C. E.; Eryazici, I.; Hauser, B. G.; Parilla, P. A.; O'Neill, K.; Sarjeant, A. A.; Nguyen, S. T.; Snurr, R. Q.; Hupp, J. T. Designing Higher Surface Area Metal−Organic Frameworks: Are Triple Bonds Better Than Phenyls? *J. Am. Chem. Soc.* **2012**, *134*, 9860−9863.
(35) Farha, O. K.; Yazaydın, A. Ö.; Eryazici, I.; Malliakas, C. D.; Hauser, B. G.; Kanatzidis, M. G.; Nguyen, S. T.; Snurr, R. Q.; Hupp, J. T. De Novo Synthesis of a Metal−Organic Framework Material Featuring Ultrahigh Surface Area and Gas Storage Capacities. *Nat. Chem.* **2010**, *2*, 944−948.
(36) Yuan, D.; Zhao, D.; Sun, D.; Zhou, H.-C. An Isoreticular Series of Metal−Organic Frameworks with Dendritic Hexacarboxylate Ligands and Exceptionally High Gas-Uptake Capacity. *Angew. Chem., Int. Ed.* **2010**, *49*, 5357−5361.
(37) Furukawa, H.; Ko, N.; Go, Y. B.; Aratani, N.; Choi, S. B.; Choi, E.; Yazaydin, A. Ö.; Snurr, R. Q.; O'Keeffe, M.; Kim, J.; Yaghi, O. M. Ultrahigh Porosity in Metal−Organic Frameworks. *Science* **2010**, *329*, 424−428.
(38) The 2017 H_2 storage targets are 5.5 wt % in gravimetric capacity, 40 g L^{-1} of volumetric capacity at an operating temperature of −40−60 °C under a maximum delivery pressure of 100 atm. See more details at http://www1.eere.energy.gov/hydrogenandfuelcells/storage/current_technology.html.
(39) Stoeck, U.; Krause, S.; Bon, V.; Senkovska, I.; Kaskel, S. A Highly Porous Metal−Organic Framework, Constructed from a Cuboctahedral Super-Molecular Building Block, with Exceptionally High Methane Uptake. *Chem. Commun.* **2012**, *48*, 10841−10843.
(40) The Advanced Research Projects Agency−Energy (ARPA-E) of the U.S. Department of Energy (DOE) has recently set new methane storage targets with the ambitious goal of a volumetric storage capacity of 350 cm^3 (STP) cm^{-3} and gravimetric storage capacity of 0.5 g (CH_4) g^{-1} (adsorbent) at room temperature. If we do not consider the adsorbent material packing loss, the new volumetric target corresponds to 263 cm^3 (STP) cm^{-3}. See DOE MOVE program at https://arpa-e-foa.energy.gov/.
(41) Chui, S. S. Y.; Lo, S. M. F.; Charmant, J. P. H.; Orpen, A. G.; Williams, I. D. A Chemically Functionalizable Nanoporous Material $[Cu_3(TMA)_2(H_2O)_3]_n$. *Science* **1999**, *283*, 1148−1150.
(42) Wu, H.; Simmons, J. M.; Liu, Y.; Brown, C. M.; Wang, X.-S.; Ma, S.; Peterson, V. K.; Southon, P. D.; Kepert, C. J.; Zhou, H.-C.; et al. Metal−Organic Frameworks with Exceptionally High Methane Uptake: Where and How is Methane Stored? *Chem.− Eur. J.* **2010**, *16*, 5205−5214.
(43) Guo, Z.; Wu, H.; Srinivas, G.; Zhou, Y.; Xiang, S.; Chen, Z.; Yang, Y.; Zhou, W.; O'Keeffe, M.; Chen, B. A Metal−Organic Framework with Optimized Open Metal Sites and Pore Spaces for High Methane Storage at Room Temperature. *Angew. Chem., Int. Ed.* **2011**, *50*, 3178−3181.
(44) Ma, S.; Sun, D.; Simmons, J. M.; Collier, C. D.; Yuan, D.; Zhou, H.-C. Metal−Organic Framework from an Anthracene Derivative

Containing Nanoscopic Cages Exhibiting High Methane Uptake. *J. Am. Chem. Soc.* **2008**, *130*, 1012−1016.
(45) Prasad, T. K.; Hong, D. H.; Suh, M. P. High Gas Sorption and Metal-Ion Exchange of Microporous Metal−Organic Frameworks with Incorporated Imide Groups. *Chem.—Eur. J.* **2010**, *16*, 14043−14050.
(46) Pan, L.; Olson, D. H.; Ciemnolonski, L. R.; Heddy, R.; Li, J. Separation of Hydrocarbons with a Microporous Metal−Organic Framework. *Angew. Chem., Int. Ed.* **2006**, *45*, 616−619.
(47) Li, B.; Wang, H.; Chen, B. Microporous Metal−Organic Frameworks for Gas Separation. *Chem.−Asian J.* **2014**, *9*, 1474−1498.
(48) Liao, P.-Q.; Zhou, D.-D.; Zhu, A.-X.; Jiang, L.; Lin, R.-B.; Zhang, J.-P.; Chen, X.-M. Strong and Dynamic CO_2 Sorption in a Flexible Porous Framework Possessing Guest Chelating Claws. *J. Am. Chem. Soc.* **2012**, *134*, 17380−17383.
(49) Chen, B.; Ma, S.; Zapata, F.; Fronczek, F. R.; Lobkovsky, E. B.; Zhou, H.-C. Rationally Designed Micropores within a Metal−Organic Framework for Selective Sorption of Gas Molecules. *Inorg. Chem.* **2007**, *46*, 1233−1236.
(50) Nugent, P.; Belmabkhout, Y.; Burd, S. D.; Cairns, A. J.; Luebke, R.; Forrest, K.; Pham, T.; Ma, S.; Space, B.; Wojtas, L.; et al. Porous Materials with Optimal Adsorption Thermodynamics and Kinetics for CO_2 Separation. *Nature* **2013**, *495*, 80−84.
(51) Chen, B.; Liang, C.; Yang, J.; Contreras, D. S.; Clancy, Y. L.; Lobkovsky, E. B.; Yaghi, O. M.; Dai, S. A Microporous Metal−Organic Framework for Gas-Chromatographic Separation of Alkanes. *Angew. Chem., Int. Ed.* **2006**, *45*, 1390−1393.
(52) Xiang, S.; Zhang, Z.; Zhao, C.-G.; Hong, K.; Zhao, X.; Ding, D.-L.; Xie, M.-H.; Wu, C.-D.; Gill, R.; et al. Rationally Tuned Micropores within Enantiopure Metal−Organic Frameworks for Highly Selective Separation of Acetylene and Ethylene. *Nat. Commun.* **2011**, *2*, 204−211.
(53) Das, M. C.; Guo, Q.; He, Y.; Kim, J.; Zhao, C.-G.; Hong, K.; Xiang, S.; Zhang, Z.; Thomas, K. M.; Krishna, R.; Chen, B. Interplay of Metalloligand and Organic Ligand to Tune Micropores within Isostructural Mixed-Metal−Organic Frameworks (M′MOFs) for Their Highly Selective Separation of Chiral and Achiral Small Molecules. *J. Am. Chem. Soc.* **2012**, *134*, 8703−8710.
(54) Chen, B.; Xiang, S.; Qian, G. Metal−Organic Frameworks with Functional Pores for Recognition of Small Molecules. *Acc. Chem. Res.* **2010**, *43*, 1115−1124.
(55) Xiang, S.; Zhou, W.; Gallegos, J. M.; Liu, Y.; Chen, B. Exceptionally High Acetylene Uptake in a Microporous Metal−Organic Framework with Open Metal Sites. *J. Am. Chem. Soc.* **2009**, *131*, 12415−12419.
(56) Xiang, S.; Zhou, W.; Zhang, Z.; Green, M. A.; Liu, Y.; Chen, B. Open Metal Sites within Isostructural Metal−Organic Frameworks for Differential Recognition of Acetylene and Extraordinarily High Acetylene Storage Capacity at Room Temperature. *Angew. Chem., Int. Ed.* **2010**, *49*, 4615−4618.
(57) Chen, B.; Ockwig, N. W.; Millward, A. R.; Contreras, D. S.; Yaghi, O. M. High H_2 Adsorption in a Microporous Metal−Organic Framework with Open Metal Sites. *Angew. Chem., Int. Ed.* **2005**, *44*, 4745−4749.
(58) Lin, X.; Telepeni, I.; Blake, A. J.; Dailly, A.; Brown, C. M.; Simmons, J. M.; Zoppi, M.; Walker, G. S.; Thomas, K. M.; Mays, T. J.; et al. High Capacity Hydrogen Adsorption in Cu(II) Tetracarboxylate Framework Materials: The Role of Pore Size, Ligand Functionalization, and Exposed Metal Sites. *J. Am. Chem. Soc.* **2009**, *131*, 2159−2171.
(59) Zhou, W.; Wu, H.; Yildirim, T. Enhanced H_2 Adsorption in Isostructural Metal−Organic Frameworks with Open Metal Sites: Strong Dependence of the Binding Strength on Metal Ions. *J. Am. Chem. Soc.* **2008**, *130*, 15268−15269.
(60) He, Y.; Krishna, R.; Chen, B. Metal−Organic Frameworks with Potential for Energy-efficient Adsorptive Separation of Light Hydrocarbons. *Energy Environ. Sci.* **2012**, *5*, 9107−9120.
(61) Bloch, E. D.; Queen, W. L.; Krishna, R.; Zadrozny, J. M.; Brown, C. M.; Long, J. R. Hydrocarbon Separations in a Metal−Organic Framework with Open Iron(II) Coordination Sites. *Science* **2012**, *335*, 1606−1610.
(62) Li, B.; Wen, H.-M.; Wang, H.; Wu, H.; Tyagi, M.; Yildirim, T.; Zhou, W.; Chen, B. A Porous Metal−Organic Framework with Dynamic Pyrimidine Groups Exhibiting Record High Methane Storage Working Capacity. *J. Am. Chem. Soc.* **2014**, *136*, 6207−6210.
(63) Zhang, Z.; Yao, Z.-Z.; Xiang, S.; Chen, B. Perspective of Microporous Metal−Organic Frameworks for CO_2 Capture and Separation. *Energy Environ. Sci.* **2014**, *7*, 2868−2899.
(64) Lin, Q.; Wu, T.; Zheng, S.-T.; Bu, X.; Feng, P. Single-Walled Polytetrazolate Metal−Organic Channels with High Density of Open Nitrogen-Donor Sites and Gas Uptake. *J. Am. Chem. Soc.* **2012**, *134*, 784−787.
(65) Xiang, S.; He, Y.; Zhang, Z.; Wu, H.; Zhou, W.; Krishna, R.; Chen, B. Microporous Metal−Organic Framework with Potential for Carbon Dioxide Capture at Ambient Conditions. *Nat. Commun.* **2012**, *3*, 954−963.
(66) Yazaydın, A. Ö.; Snurr, R. Q.; Park, T.-H.; Koh, K.; Liu, J.; LeVan, M. D.; Benin, A. I.; Jakubczak, P.; Lanuza, M.; Galloway, D. B.; et al. Screening of Metal−Organic Frameworks for Carbon Dioxide Capture from Flue Gas Using a Combined Experimental and Modeling Approach. *J. Am. Chem. Soc.* **2009**, *131*, 18198−18199.
(67) Demessence, A.; D'Alessandro, D. M.; Foo, M. L.; Long, J. R. Strong CO_2 Binding in a Water-Stable, Triazolate-Bridged Metal−Organic Framework Functionalized with Ethylenediamine. *J. Am. Chem. Soc.* **2009**, *131*, 8784−8786.
(68) Nguyen, N. T. T.; Furukawa, H.; Gándara, F.; Nguyen, H. T.; Cordova, K. E.; Yaghi, O. M. Selective Capture of Carbon Dioxide under Humid Conditions by Hydrophobic Chabazite-Type Zeolitic Imidazolate Frameworks. *Angew. Chem., Int. Ed.* **2014**, *53*, 10645−10648.
(69) Sato, H.; Kosaka, W.; Matsuda, R.; Hori, A.; Hijikata, Y.; Belosludov, R. V.; Sakaki, S.; Takata, M.; Kitagawa, S. Self-Accelerating CO Sorption in a Soft Nanoporous Crystal. *Science* **2014**, *343*, 167−170.
(70) Bétard, A.; Bux, H.; Henke, S.; Zacher, D.; Caro, J.; Fischer, R. A. Fabrication of a CO_2-Selective Membrane by Stepwise Liquid-phase Deposition of an Alkylether Functionalized Pillared-layered Metal−Organic Framework $[Cu_2L_2P]_n$ on a Macroporous Support. *Microporous Mesoporous Mater.* **2012**, *150*, 76−82.
(71) He, Y.; Zhou, W.; Qian, G.; Chen, B. Methane Storage in Metal−Organic Frameworks. *Chem. Soc. Rev.* **2014**, *43*, 5657−5678.